Detecting Power Voltage Dips Using Tracking Filters - A Comparison Against Kalman

Ion R. STANCIU[1], Florin MOLNAR-MATEI[2]
[1]*Politehnica University of Timisoara, Department of Hydraulic Machinery, 300222, Romania*
[2]*Politehnica University of Timisoara, Power Engineering Department, 300223, Romania*
rares.stanciu@mh.mec.upt.ro

***Abstract*—Due of its significant economical impact, Power-Quality (PQ) analysis is an important domain today. Severe voltage distortions affect the consumers and disturb their activity. They may be caused by short circuits (in this case the voltage drops significantly) or by varying loads (with a smaller drop). These two types are the PQ currently issues. Monitoring these phenomena (called dips or sags) require powerful techniques. Digital Signal Processing (DSP) algorithms are currently employed to fulfill this task. Discrete Wavelet Transforms, (and variants), Kalman filters, and S-Transform are currently proposed by researchers to detect voltage dips.**

This paper introduces and examines a new tool to detect voltage dips: the so-called tracking filters. Discovered and tested during the cold war, they can estimate a parameter of interest one-step-ahead based on the previously observed values. Two filters are implemented. Their performance is assessed by comparison against the Kalman filter's results.

***Index Terms*—Power Quality, Voltage Dips, Digital Signal Processing, Tracking Filters, Kalman Filters.**

I. INTRODUCTION

As the society evolves, the electricity demands increase. The population number and their needs have grown. Consequently, the industrial development which is expected to support people needs has demanded large power networks. Electricity-producing plants, transformers, and high-voltage lines are elements that form modern power systems. The PQ on these networks continues to be a major concern for many industrial customers. Several categories of events can occur in these power networks during every-day operation. The toughest event is the short circuit which may result in total power disruption. Voltage reductions may be caused by short circuits (and in these cases they are severe) or by varying loads [1]. These phenomena are known as "voltage dips" or "voltage sags" in the PQ domain. Simply said, these are Root-Mean-Square (RMS) voltage variations (considering three-phase systems) which affect the industrial consumers. According to Gallo [2], these events end due to the automatic switching, load stabilization and/or power system actions. However, they are considered important issues [3].

Standards define voltage dips as one of the most important aspects of power quality [4]. Common ways to characterize these phenomena have to be established. They are considered of rectangular shape, characterized by magnitude and duration [4]. Commonly, the dip's magnitude is defined to be the voltage reduction under the 90% threshold [4]. If the voltage falls below 10%, the perturbation is considered to be an interruption. A typical voltage dip shape can be seen in Fig. 1. The duration of the event is the time measured from the moment when RMS voltage drops below the 90% threshold to the moment it rises above it. Possible values range from few power cycles (tens of milliseconds) to one minute. Balanced dips are many times assumed in three-phase power systems. In reality, most voltage dips occur due to unbalanced faults, which introduce different values of voltage for each phase and phase angle shift [1].

The IEC Standard [5] describes a procedure for dip detection. According to this procedure, the RMS voltage is compared against a threshold (usually a percentage) which is typically 90% of the nominal RMS. One cycle of acquired data is used to compute the RMS voltage. The IEC standard defines the RMS voltage to be the root mean square value of the AC signal measured over one cycle and commencing at zero-crossing. Unfortunately, the zero-crossing moments are not reliable during a voltage dip.

Two problems have to be addressed for dip characterization: 1) to establish which voltages will be measured – phase to phase or phase to neutral and 2) to establish the DSP technologies to be employed. Didden [6] and Leborgne et al [7] have studied these connections for voltage measurement. Despite the fact that the two articles have different purpose, they underline pros and cons for both voltage measurement connections. However, since most of the recorders are connected between phase and neutral, it is recommended to use this connection type.

In literature, there are many DSP technologies employed for voltage dip detection. Many of them use different types of wavelet transforms or Kalman filters [3], [8], [9], [10], [11], [12]. Literature analysis reveals that wavelet transform is preferred when the dips are targeted together with other PQ problems.

Styvaktalcis et al [13] performed a comparative study in using four methods for RMS computation: the RMS value calculated over one-cycle overlapping windows, the RMS value calculated over half-cycle overlapping windows, Kalman filter of order 20 and Kalman filter order 1 cascaded with a low-pass filter. They conclude that the speed of detection depends for each method on the voltage dip magnitude, the point where the dip starts (on the wave) and the phase angle jump that is caused.

This paper was supported by the project "Development and support for multidisciplinary postdoctoral programs in major technical areas of national strategy for Research – Development – Innovation" 4D-POSTDOC, contract nr. POSDRU/89/1.5/S/52603, project co-funded by the European Social Fund through Sectorial Operational Program Human Resources Development 2007-2013.

Digital Object Identifier 10.4316/AECE.2012.04012

Barros and Perez [3] have proposed the Kalman filters to monitor events on a three-phase voltage system. Three Kalman filters running on a DSP structure are used to monitor the three RMS voltages periodically calculated from sampling voltage values. Their experimental results reveal a suitable method for automatic detection.

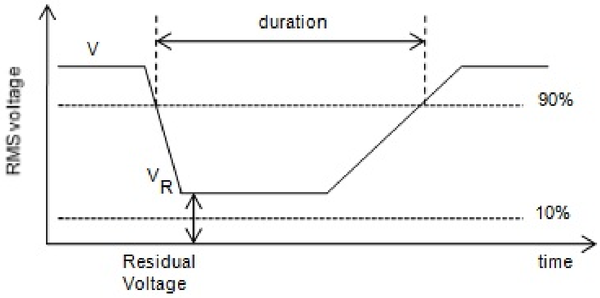

Figure 1: A typical voltage dip and its parameters

The same authors [11] took a step further and have proposed an Extended Kalman Filter for dip detection. They have compared the results with the RMS calculated using the half-cycle overlapping windows. However, the comparison against the classical Kalman filter was not performed. Perez and Barros have also developed a software platform for PQ analysis [12]. The implemented algorithms are: the r.m.s magnitude, the Fourier analysis, the Kalman filtering and the wavelet analysis.

Dash et al [8] have used the same Extended Kalman Filter for frequency measurement. They demonstrate that the frequency and amplitude can be estimated in the same time. Dash et al have addressed two problems: the tracking frequency and the tracking voltage amplitude. In 2004 Dash et al [9] have extended the Kalman filter use by combining it with the S-Transform. The latter was needed for perturbation detection while Kalman filter was employed to extract data for event characterization.

A combination of Kalman, discrete wavelet transform and artificial intelligence (fuzzy expert system) was proposed in [14]. The discrete wavelet transform was used to improve the Signal-Noise Ratio (SNR) while the Kalman filter extracted the needed information. The fuzzy system was employed to analyze the data for power quality characterization.

A better RMS detection was proposed by Reddy in [15] by using an Unscented Kalman filter combined with artificial intelligence techniques for fast tracking of the power quality disturbance. The authors compare the algorithm with the Extended Kalman filter and demonstrate the superiority of their results.

During the sudden RMS reduction, the dip distorts the sinusoidal wave, therefore introducing harmonics. Santoso et al [16] have proposed a dyadic-orthonormal wavelet transform for PQ disturbances. Their key idea was to decompose the disturbance into other signals using the Multi-Resolution Signal Decomposition technique. The wavelet transform proved to be a powerful tool. However, the mother wavelet selection played an important role in detecting disturbance.

An alternative detection algorithm based on the Generalized Likelihood Ratio Test (GLRT) was proposed by Guerrieri et al in [17]. Their approach can achieve competitive statistical performance when smooth transients are associated to the voltage dips.

A probabilistic approach has also been used in power quality analysis [10], [18] and [19]. A slow-enough disturbance variation which does not affect the process accuracy was assumed.

Oftentimes, the voltage dip detectors are built using embedded hardware (DSP or microcontroller-based). When operating, its main tasks include data acquisitions and analog to digital conversion, RMS calculation (several previously-sampled voltage values stored in the memory are used), signal processing for dip detection and eventually, recording the event (for log files) and alert issuing. Since the dip can occur on any phase, a three-phase watching is indicated. However, in such a case the amount of work triples. A DSP board (which offers a significant computation power) is preferred (instead of a microcontroller) for this task [3]. As such, any possible algorithm simplification or increase in computational power is therefore useful.

This paper introduces and examines a new algorithm for voltage dip detection: the α–β–γ filter. The reason behind this approach lies on its simplicity. The proposed filter is simpler than Kalman due to the fact that it has constant coefficients. The objective of this paper is to assess its performance by comparison to the Kalman filter. Section II of this paper introduces this family of filters and describes the α–β–γ filter. Section III discusses the filter's stability using the Jury' stability criterion (presented as well). Section IV presents the theory behind the Kalman filter. The two filters are applied to real data for 110kV power line and the results of the two filters are compared in Section V.

II. The Alpha-Beta Family of Tracking Filters

The IT technologies have brought significant transformations to our life. Indeed, about a hundred microprocessors can be found today a modern home. Numerous real-life applications use digital data today. It is almost impossible to imagine a fully-analog device today.

Civilian and military applications such as the air-traffic handling, the missile interception and the anti-submarine warfare require the use of discrete-time data to predict the kinematics of a moving object. The use of passive sonobuoys which have limited power capacity pushes for implementation of computationally inexpensive target-trackers.

The α–β family of filters was developed in the cold-war era by Sklansky [20]. At that time, it was intended for radar target tracking, position and velocity estimation from noisy measurements of range and bearing. Since then, they have been used for both predictions and tracking. Kalata and Murphy [21] have tried to use them for tracking with rate variations. Tenne and Singh [22] have studied ways to design them for optimal performance. In their work they also indicate how to select the parameters to obtain a stable filter. Corke and Good [23] have compared their performance with Kalman filters in the computer vision domain. They have underlined that in case of using Kalman filters the coefficients will converge to constant values. In their case, the α–β–γ filters delivered similar performance with less computational effort. Stanciu and Oh [24] have employed these filters in visual servoing to predict one-step-ahead the target's position in their image plane.

The Tracking Filters

There are two algorithms in this family. Both of them are working in two steps: prediction and correction.

The one examined in this work is the extended version in the family called the α–β–γ filter. In the prediction step, this algorithm estimates one-step-ahead the position and velocity. In the correction step the filter is smoothing the position, the velocity, and the acceleration and improves the tracking performance. The predicted values (the position (1) and the velocity (2)) for iteration *k+1* which are written as functions of the current smoothed values for position, velocity, accelerations and the sampling time T.

$$x_p(k+1) = x_s(k) + T \cdot v_s(k) + \frac{T^2}{2} \cdot a_s(k) \tag{1}$$

$$v_p(k+1) = v_s(k) + T \cdot a_s(k) \tag{2}$$

The position, the velocity and the acceleration are then corrected (smoothed) based on the observed position $x_0(k)$ at iteration *k* in Eqs. (3), (4) and (5).

$$x_s(k) = x_p(k) + \alpha \cdot \left[x_o(k) - x_p(k)\right] \tag{3}$$

$$v_s(k) = v_p(k) + \frac{\beta}{T} \cdot \left[x_o(k) - x_p(k)\right] \tag{4}$$

$$a_s(k) = a_s(k-1) + \left(\frac{\gamma}{2 \cdot T^2}\right) \cdot \left[x_o(k) - x_p(k)\right] \tag{5}$$

III. The Stability of the Alpha-Beta-Gamma Filter

Prior to its implementation a stability study was performed. The objective was to determine the parameter ranges (for α, β, and γ) which ensure a stable filter. To obtain the transfer function (which relates the two positions - predicted and observed) one has to apply the Z-transform to the prediction and the correction equations. By applying it to the prediction equations one ends up with:

$$zX_p(z) - zx_p(0) = X_s(z) + TV_s(z) + \frac{1}{2}T^2 A_s(z) \tag{6}$$

$$zV_p(z) - zv_p(0) = V_s(z) + TA_s(z) \tag{7}$$

By applying the Z-transform to the correction equations one ends up with:

$$X_s(z) = X_p(z) + \alpha \cdot \left[X_o(s) - X_p(z)\right] \tag{8}$$

$$V_s(z) = V_p(z) + \frac{\beta}{T} \cdot \left[X_o(s) - X_p(z)\right] \tag{9}$$

$$A_s(z) = \frac{1}{z} \cdot A_s(z) + \left(\frac{\gamma}{2 \cdot T^2}\right) \cdot \left[X_o(s) - X_p(z)\right] \tag{10}$$

In (10), the term *1/z* takes into account the fact that $a_s(k-1)$ is the former value of acceleration (for iteration *k-1* – Eq. (10)). By applying the Z-transform the smoothed acceleration becomes:

$$A_s(z) = \left(\frac{z}{z-1}\right) \cdot \left(\frac{\gamma}{2 \cdot T^2}\right) \cdot \left[X_o(s) - X_p(z)\right] \tag{11}$$

To derive the position transfer function, in (6) and (7) the smoothed speed and acceleration $V_s(z)$ and $A_s(z)$ are replaced by (9) and (10). The predicted position becomes:

$$\begin{aligned} z \cdot X_p(z) &= z \cdot x_p(0) + X_p(z) + \alpha \cdot \left[X_o(s) - X_p(z)\right] + \\ &+ T \cdot \left[V_p + \frac{\beta}{T} \cdot \left(X_o(s) - X_p(z)\right)\right] + \\ &+ \frac{1}{4} \cdot \frac{z}{z-1} \cdot \gamma \cdot \left[X_o(s) - X_p(z)\right] \end{aligned} \tag{12}$$

If assuming $v_p(0)=0$, the predicted velocity becomes:

$$V_p(z) = \frac{1}{T} \cdot \left[X_o(s) - X_p(z)\right] \cdot \left[\frac{2 \cdot \beta(z-1) + \gamma \cdot z}{2 \cdot (z-1)^2}\right] \tag{13}$$

Substituting the predicted velocity given by (13) into (12) yields to:

$$\begin{aligned} (z-1)X_p(z) &= z \cdot x_p(0) + \left[X_0(z) + X_p(z)\right] \cdot \\ &\cdot \left[\alpha + \frac{2 \cdot \beta \cdot (z-1) + \gamma \cdot z}{2 \cdot (z-1)^2} + \beta + \frac{1}{4} \cdot \frac{z}{z-1} \cdot \gamma\right] \end{aligned} \tag{14}$$

Assuming $x_p(0)=0$, the obtained equation depend on $X_p(z)$, $X_0(z)$ and the parameters α, β, and γ. Therefore, the transfer function relating the predicted and the observed position is given by (15) (where "P" stands for position):

$$\begin{aligned} G_{P\alpha\beta\gamma}(z) &= \frac{X_p(z)}{X_0(z)} = \\ &\frac{\left(\alpha + \beta + \frac{\gamma}{4}\right) \cdot z^2 + \left(-2 \cdot \alpha - \beta + \frac{\gamma}{4}\right) \cdot z + \alpha}{z^3 + \left(\alpha + \beta + \frac{\gamma}{4} - 3\right) \cdot z^2 + \left(-2 \cdot \alpha - \beta + \frac{\gamma}{4} + 3\right) \cdot z + \alpha - 1} \end{aligned} \tag{15}$$

For voltage dip detection, the predicted "position" is assumed to be the RMS voltage at next iteration. Another transfer function relating the predicted "velocity" to the observed position can be derived. However, the voltage rate of change (which corresponds to the "velocity" parameter of the tracking filter) was not examined in this work.

The Jury's Stability Criterion

A stability criterion is needed to examine the filter stability. Since the z-plane's boundary is different that of the s-plane, the Routh-Hurwitz stability criterion cannot be applied directly. However, a similar method but for discrete systems is represented by the Jury's stability test. This is used in the following to study the filter's stability. A table is constructed based on the coefficients of the characteristic polynomials.

Considering the characteristic equation of a discrete-time system to be the one expressed by (16).

$$G(z) = a_n \cdot z^n + a_{n-1} \cdot z^{n-1} + \ldots + a_1 \cdot z + a_0 \tag{16}$$

The Jury's stability test is formed as shown in Table I.

TABLE I. THE JURY'S STABILITY TABLE

z^0	z^1	…	z^{n-1}	z^n
a_0	a_1	…	a_{n-1}	a_n
a_n	a_{n-1}	…	a_1	a_0
b_0	b_1	…	b_{n-1}	
b_{n-1}	b_{n-2}	…	b_1	
c_0	c_1	…		
c_{n-2}	c_{n-3}	…		
…	…	…		
m_0	m_1	m_2		

The Table I contains one row only if a second order system is examined. Two rows are added to the table for each additional order increase. The even-numbered rows have the same elements as the previous rows but in reversed order. The odd-numbered rows have their elements defined as can be seen in (17) and (18).

$$b_k = \begin{vmatrix} a_0 & a_{n-k} \\ a_n & a_k \end{vmatrix} \quad (17)$$

$$c_k = \begin{vmatrix} b_0 & b_{n-1-k} \\ b_{n-1} & b_k \end{vmatrix} \quad (18)$$

The polynomial *G(z)* defined by (16) has no roots outside the unit circle (or on its border) if the *n-1* following constraints are satisfied [25].

$$G(1) > 0 \quad (19)$$

$$(-1)^n \cdot G(-1) > 0 \quad (20)$$

$$|a_0| < |a_n| \quad (21)$$

$$|b_{n-1}| < |b_0| \quad (22)$$

$$|c_{n-2}| < |c_0| \;\; \ldots \;\; |m_2| < |m_0| \quad (23)$$

The conditions expressed by (19) and (20) are sometimes called the *necessary stability conditions*. The conditions expressed by (21), (22) and (23) are sometimes know as the *sufficient stability conditions*.

The characteristic polynomials coefficients for the filter's position can be seen in Table II.

TABLE II. THE JURY'S STABILITY TEST TABLE FOR THE FILTER

z^0	z^1	z^2	z^3
$\alpha-1$	$-2\cdot\alpha-\beta+\frac{\gamma}{4}+3$	$\alpha+\beta+\frac{\gamma}{4}-3$	1
1	$\alpha+\beta+\frac{\gamma}{4}-3$	$-2\cdot\alpha+\beta+\frac{\gamma}{4}+3$	$\alpha-1$
$\alpha(\alpha-2)$	$\alpha\left(4-2\cdot\alpha-\beta+\frac{\gamma}{4}\right)-\frac{1}{2}$	$\alpha\left(\alpha+\beta-2+\frac{\gamma}{4}\right)-\frac{1}{2}$	

For the first necessary stability condition, is then:

$$1+\alpha+\beta+\frac{\gamma}{4}-3-2\cdot\alpha-\beta+\frac{\gamma}{4}+3+\alpha-1=\frac{\gamma}{2}>0 \quad (24)$$

Eq. (24) simply restricts the parameter γ to positive values. The second necessary stability condition translates to:

$$2\cdot\alpha+\beta<4 \quad (25)$$

There are two sufficient stability conditions to be fulfilled. Since a_0 is one, Eq. (21) translates to:

$$|\alpha-1|<1 \quad (26)$$

This is equivalent to:

$$0<\alpha<2 \quad (27)$$

The second condition which ensures stability is:

$$|\alpha\cdot(\alpha-2)| > \left|\alpha\cdot(\alpha-2)+\alpha\cdot\left(\beta+\frac{\gamma}{4}\right)-\frac{\gamma}{2}\right| \quad (28)$$

According to (27) the parameter α is always positive and the quantity *(α-2)* is always negative. This leads to:

$$\alpha\cdot\left(\beta+\frac{\gamma}{4}\right)-\frac{\gamma}{2}>0 \quad (29)$$

Eq. (29) translates to:

$$\gamma<\frac{4\cdot\alpha\cdot\beta}{2-\alpha} \quad (30)$$

Two α–β–γ filters were implemented and tested by comparison against both the Kalman filter results and each other. The two filters have the following parameters (Table III). Both sets of parameters satisfy the above-determined conditions.

TABLE III. THE PARAMETERS OF THE TWO TRACKING FILTERS IMPLEMENTED AND TESTED

1st tracking filter	2nd tracking filter
$\alpha_1=0.75$	$\alpha_2=0.75$
$\beta_1=0.8$	$\beta_2=2$
$\gamma_1=0.25$	$\gamma_2=1,5$

IV. THE KALMAN FILTER

The α–β–γ filter was implemented with the above values for the parameters. Power data was used to test and compare the results of the filter by comparison to the Kalman filter (which was also implemented).

The so-called "Kalman filters" were developed by Kalman in the 60s [26]. Since then, their area of application has grown considerably. Matthies and Kanade [27] use this algorithm to estimate depth from image sequences. Mohamed and Schwarz [28] use adaptive Kalman filtering for Global Positioning System.

This algorithm is a way to estimate the state $x \in \Re^n$ of a discrete-time controlled process governed by (31).

$$x_k = A\cdot x_{k-1} + B\cdot u_{k-1} + w_{k-1} \quad (31)$$

where A is a square matrix relating the previous state x_{k-1} to the actual state x_k, u_{k-1} is the control variable and the w_{k-1} is the noise. The measurement can be expressed as (32) shows.

$$z_k = H\cdot x_k + v_k \quad (34)$$

Here, v_k is the noise affecting the measurements, and the *m x n* matrix *H* relates the measurement to the state x_k. The a priori and a posteriori estimate errors given by the measurement at iteration *k* are expressed by (33) and (34).

$$e_k^- = x_k - \hat{x}_k^- \quad (33)$$

$$e_k = x_k - \hat{x}_k \quad (34)$$

Here, the $\hat{x}_k^-$ and the $\hat{x}_k$ are the a priori and a posteriori estimates for iteration *k*. The a priori and a posteriori estimate error covariances are defined [29] as below:

$$P_k^- = E\left[e_k^- e_k^{-T}\right] \quad (35)$$

$$P_k = E\left[e_k e_k^T\right] \quad (36)$$

The estimate error covariance is given by equation (37), where $E\left(\hat{X}_{k+1}\right)$ is the first order moment.

$$P_{k+1} = E\left[\left(\hat{X}_{k+1} - E\left(\hat{X}_{k+1}\right)\right)^2\right] \quad (37)$$

By substituting the first order moment and considering $\hat{X}_k$ and Z_k independent variables, the estimate error covariance is then:

$$P_{k+1} = (1-K)^2\cdot P_k + K^2\cdot R_{k+1} \quad (38)$$

The best estimation is obtained by taking the derivative with respect to K and forces it to be zero.

$$K_k = \frac{P_k}{P_k + R_{k+1}} \tag{39}$$

The estimate error covariance is then:

$$P_{k+1} = \frac{P_k \cdot R_{i+1}}{P_k + R_{k+1}} = \left(1 - K_k\right) P_k \tag{40}$$

The Kalman filter was implemented as shown in Table IV.

TABLE IV. THE KALMAN FILTER'S EQUATIONS

Prediction	Correction
$\hat{x}_k^- = \hat{x}_{k-1}$ $P_k^- = P_{k-1}$	$K_k = \frac{P_k^-}{P_k^- + R}$ $\hat{x}_k = \hat{x}_k^- + K_k\left(z_k - \hat{x}_k^-\right)$ $P_k = \left(1 - K_k\right) P_k^-$

V. Simulations and Results

The first assessment of the two criteria took into consideration how fast the two algorithms are able to detect a voltage dip. Both filters target the RMS voltage. The power voltage is sampled 20 times/cycle which results in a sampling frequency of 1000Hz. The RMS voltage is computed using (43).

$$V_{RMS}\left(k\right) = \sqrt{\sum_{i=k-20}^{k} \left(v\left(i\right)\right)^2} \tag{41}$$

Here, *v(i)* is the i^{th} sample (one of the last 20^{th} samples). The last 20 samples are used to compute the actual RMS voltage. Consequently, a three-phase system triples the work to be done. This may be inconvenient when using an embedded hardware platform (a microcontroller) because the unit has to sample the three phase voltages, compute the RMS values for all three of them, and then run dip-detection algorithms.

After filter implementation it was interesting to assess its voltage dip detection performance. Data corresponding to 110kV power line was used for this purpose. This test attempts to assess the "α–β–γ" voltage dip detection speed using real-time data.

The time interval T is 1ms (corresponding to a sampling frequency of 1000Hz) so there are 20 samples for each power cycle. As it can be seen in Fig. 2, the voltage on phase T decreases suddenly by half at the very beginning of the fourth power network cycle. The filter's predicted value for phase T and the RMS 90% threshold can be seen in Fig. 3. It can be seen that the prediction drops to 90% in less than a quarter of a cycle (5 ms for a 50Hz power network).

For the Kalman filter implementation, the matrices A and H were set to 1. A deviation value of 0.001 was chosen. The filter's equations are shown in Table IV. For comparison, the Kalman filter is used to detect the same dip (Fig. 2) as the tracking filters. In this case, the difference between the nominal and actual RMS voltages is compared with the 10% threshold (Fig. 4).

Another tracking filter was implemented using the second set of parameters (Table III). The detecting time of the latest filter is the lowest (Fig. 5). Its voltage dip detection time is reduced to 0.1 of a network cycle (2 ms). A detail can be seen in Fig. 6. This suggests that "α–β–γ" is a very sensitive tool to detect such events.

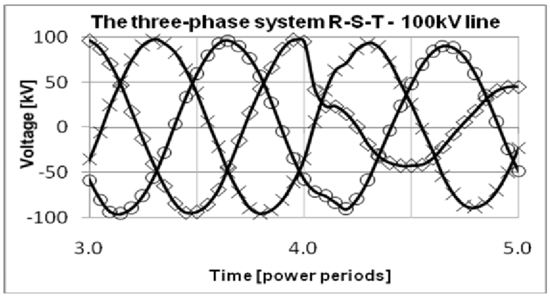

Figure 2: Three-phase power network voltage dip

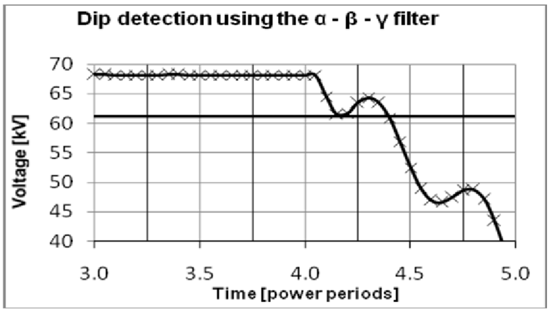

Figure 3: Three-phase power network voltage dip using the first tracking filter

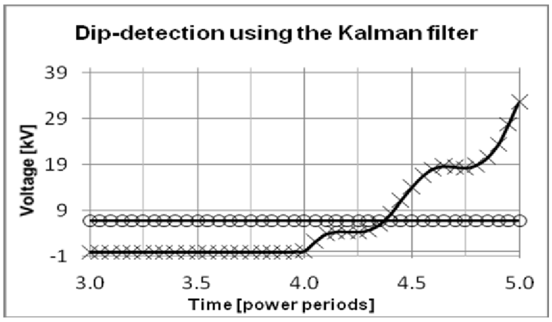

Figure 4: Three-phase power network voltage dip using the Kalman filter

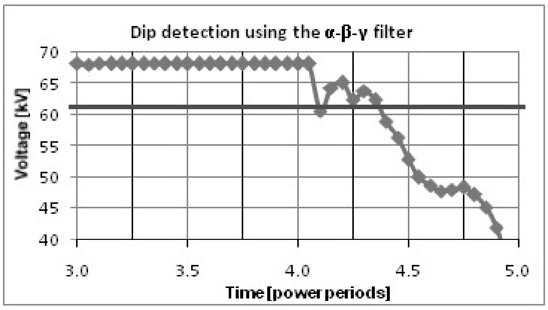

Figure 5: Three-phase power network voltage dip using the second tracking filter

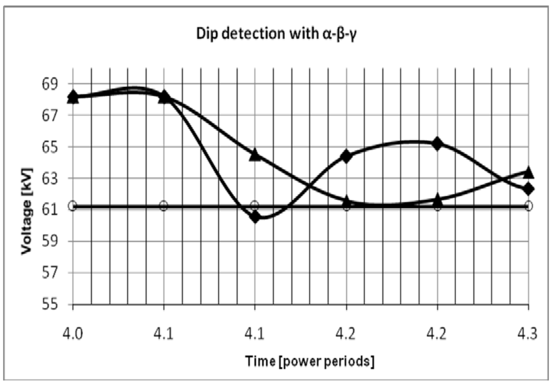

Figure 6: Power network voltage dip detection with two tracking filters (Table III): the second filter delivers better detection performance

VI. Conclusion and Future Work

Voltage dips are undesired phenomena affecting the power quality. They are regarded to be the main issue in power quality today. Digital signal processing techniques like Kalman filters and Discrete Wavelet transforms were proposed to detect them.

To perform detection, the voltage is sampled by the digital system. The RMS value has to be computed using several sampled values. A detection algorithm has to be employed to detect these events. If this computation has to be done for a three-phase system, the amount of work triples. Consequently, any computation reduction is useful.

This paper proposes a new method for voltage dips detection. Called the α–β–γ filter, this algorithm is simpler than Kalman because it has constant coefficients, thus reducing the amount of computation. After describing the members of the family, the stability is analyzed using the Jury's criterion. This way, the possible interval values for filter's parameters is determined. Its performance is tested on real-data by comparison to the Kalman filter. The proposed algorithm detects the dips faster than Kalman. It can be tuned to obtain even better performance. However, there is an inconvenience: it still uses the RMS values, which have to be computed for all three phases. This aspect is going to be addressed in future work.

References

[1] M. H. J. Bollen, *Understanding Power Quality Problems. Voltage Sags and Interruptions*. NY: IEEE Press, New York, 2000.

[2] D. Gallo, C. Landi, M. Luiso, "Accuracy Analysis of Algorithms Adopted in Voltage Dip Measurements", IEEE Trans. on Instrumentation and Measurement, Vol. 59, No. 10, pp. 2652-2659, Oct. 2010. [Online]. Available: http://dx.doi.org/10.1109/TIM.2010.2045256

[3] J. Barros, E. Perez, "Automatic Detection and Analysis of Voltage Events in power Systems", IEEE Transactions on Instrumentation and Measurement, Vol. 55, No. 5, pp. 1487-1493, Sept. 2006. [Online]. Available: http://dx.doi.org/10.1109/TIM.2006.881584

[4] EN 50160:2007, Voltage Characteristics of Electricity Supplied by Public Distribution Networks

[5] Electromagnetic Compatibility (EMC) Part 4-30: Testing and Measurement Techniques—Power Quality Measurement Methods, IEC 61000-4-30, 2003.

[6] M. Didden, E. De Jaeger, W. D'Haeseleer, R. Belmans, "How to connect a voltage sag-measuring device: Phase to phase or phase to neutral?", IEEE Trans. on Power Delivery, vol. 20, no. 2, pp. 1174–1181, Apr. 2005. [Online]. Available: http://dx.doi.org/10.1109/TPWRD.2004.834855

[7] R. C. Leborgne, G. Olguin, M. H. J. Bollen, "The Influence of PQ-Monitor Connection on Voltage Dip Measurements", *Proceedings of IEE MedPower Conference*, Nov. 2004, Cyprus.

[8] P. K. Dash, R. K. Jena, G. Panda, A. Routray, "An Extended Complex Kalman Filter for Frequency Measurement of Distorted Signals", IEEE Trans. on Instrumentation and Measurement, Vol. 49, No. 4, pp. 746-753, Aug. 2000. [Online]. Available: http://dx.doi.org/10.1109/19.863918

[9] P. K. Dash, M. V. Chilukuri, "Hybrid S-Transform and Kalman Filtering Approach for Detection and Measurement of Short Duration Disturbances in Power Networks", IEEE Trans. on Instrumentation and Measurement, Vol. 53, No. 2, pp. 588-596, Apr. 2004. [Online]. Available: http://dx.doi.org/10.1109/TIM.2003.820486

[10] I. Y. Gu, E. Styvaktakis, "Bridge the gap: Signal processing for power quality applications", Electric Power System Research, vol. 66, no. 1, pp. 83-96, Jul. 2003. [Online]. Available: http://dx.doi.org/10.1016/S0378-7796(03)00074-9

[11] E. Perez, J. Barros, "An extended Kalman filtering approach for detection and analysis of voltage dips in power systems", Electric Power Systems Research, vol. 78, pp. 618–625, Apr. 2008. [Online]. Available: http://dx.doi.org/10.1016/j.epsr.2007.05.006

[12] E. Perez, J. Barros, "Application of advanced digital signal processing tools for analysis of voltage events in power systems", International Journal of Electrical Engineering Education, Vol. 46, No. 3, pp. 211-224, Jul. 2009.

[13] E. Styvaktalcis, I. Y. Gu, M. H. J. Bollen, "Voltage Dip Detection and Power System Transients", *Power Engineering Society Summer Meeting*, Vancouver, Canada, 15-19 Jul. 2001, pp. 683-688. [Online]. Available: http://dx.doi.org/10.1109/PESS.2001.970124

[14] A. A. Abdelsalam, A. A. Eldesouky, A. A. Sallam, "Characterization of power quality disturbances using hybrid technique of linear Kalman filter and fuzzy-expert system", Electric Power System Research, vol. 83, pp. 41-50, Feb. 2011. [Online]. Available: http://dx.doi.org/10.1016/j.epsr.2011.09.018

[15] J. B. V. Reddy, P. K. Dash, R. Samantaray, A.K. Moharana, "Fast Tracking of Power Quality Disturbance Signals Using an Optimized Unscented Filter", IEEE Transactions on Instrumentation and Measurement, Vol. 58, No. 12, pp. 3943-3952, Dec. 2009. [Online]. Available: http://dx.doi.org/10.1109/TIM.2009.2020835

[16] S. Santoso, E. J. Powers W. M. Grady, P. Hofman, "Power quality assessment via wavelets transform analysis," IEEE Trans. on Power Delivery, Vol. 11, No. 2, pp. 924-930, Apr. 1996. [Online]. Available: http://dx.doi.org/10.1109/61.489353

[17] G. Guerrieri, A. Moschitta, P. Carbone, C. Muscas, "Statistical Properties of Voltage Dip Detectors", IEEE Trans. on Instrumentation and Measurement, Vol. 59, No. 11, pp. 2800-2807, Jul. 2010. [Online]. Available: http://dx.doi.org/10.1109/AMUEM.2009.5207598

[18] R. A. Flores, "State of the art in the classification of power quality events, an overview" , in *Proc. 10th International Conference Harmonics Quality of Power*, vol. 1, pp. 17-20, 2002. [Online]. Available: http://dx.doi.org/10.1109/ICHQP.2002.1221398

[19] W. R. A. Ibrahim, M. M. Morcos, "Artificial intelligence and advanced mathematical tools for power quality applications: A survey", IEEE Trans. on Power Delivery, vol. 17, no. 2, pp. 668-673, Apr. 2002. [Online]. Available: http://dx.doi.org/10.1109/61.997958

[20] J. Sklansky, *Optimizing the dynamic parameter of a track-while-scan system*, RCA Laboratories, Princeton, NJ, June 1957.

[21] P. R. Kalata, K. M. Murphy, "α-β target tracking with track rate variations", in *Proceedings of 29th Southeastern Symposium on System Theory*, 1997, pp. 70-74. [Online]. Available: http://dx.doi.org/10.1109/SSST.1997.581581

[22] D. Tenne, T. Singh, "Optimal design of α-β-(γ) filters", in *Proceedings of American Control Conference*, Chicago, Illinois, 2000, vol. 6, pp. 4348-4352. [Online]. Available: http://dx.doi.org/10.1109/ACC.2000.877043

[23] P. I. Corke, M. C. Good, "Dynamic effects in high-performance visual servoing", in *International Conference on Robotics and Automation*, Nice, France, 1992, pp. 1838-1843. [Online]. Available: http://dx.doi.org/10.1109/ROBOT.1992.219960

[24] R. Stanciu, P. Y. Oh, "Human-in-the-loop Camera Control for a Mechatronic Broadcast Boom", IEEE/ASME Transactions on Mechatronics, Vol. 12, Issue 1, pp. 41 – 52, Feb. 2007. [Online]. Available: http://dx.doi.org/10.1109/TMECH.2006.886252

[25] C. L. Phillips, H. T. Nagle, *Digital Control System Analysis and Design, Third Edition*, Prentice Hall, 1995.

[26] R. E. Kalman, "A New Approach to Linear Filtering and Prediction Problems", Transaction of the ASME – Journal of Basic Engineering, pp. 35-45, 1960.

[27] L. Matthies, T. Kanade, "Kalman Filter-based Algorithms for Estimating Depth from Image Sequences", International Journal of Computer Vision, vol. 3, pp. 209-236, Sep. 1989. [Online]. Available: http://dx.doi.org/10.1007/BF00133032

[28] H. Mohamed, K. P. Schwarz, "Adaptive Kalman Filtering for INS/GPS", Journal of Geodesy, vol. 73, no. 4, pp. 193-203, 1999. [Online]. Available: http://dx.doi.org/10.1007/s001900050236

[29] G. Welch, G. Bishop, *An Introduction to the Kalman Filter*, SIGGRAPH Chapel Hill, 2000.